

## NUMERICAL INVESTIGATION OF HEAD DIAMETER INFLUENCE ON TENSILE CAPACITY OF HEADED STUDS

Jindřich Fornůsek\* & Petr Konvalinka

*Experimental Centre Faculty of Civil Engineering, CTU in Prague,  
Prague, Czech Republic*

\*Corresponding author: [jindrich.fornusek@fsv.cvut.cz](mailto:jindrich.fornusek@fsv.cvut.cz)

---

**Abstract:** Objective of this paper is comparison of results of numerical analysis of headed studs with different head size and CCD (Concrete Capacity Design) approach which is used for design of anchoring in Eurocode 2. The breakout simulation tests of six different head diameters with four different effective embedment depths were investigated. The concrete properties were kept constant for all of them. It was found that the capacity of anchor is affected by the head size significantly. The approximately 25% decrease of capacity for small heads and about 30% capacity increase for large heads were observed in comparison to the CCD method.

**Keywords:** *Anchorage, Breakout Capacity, Concrete, Headed Studs, Numerical Simulation, Tension.*

### 1.0 Introduction

The anchorage systems for concrete structures are well known and tested especially in bridge engineering where anchors transfer the shear load from steel girders to concrete slabs. Demands of designers for new fast and flexible technologies of concrete reinforcing and casting moved the anchorage systems to another application like tension and combination of tension and shear in common concrete structures. Therefore deeper investigation of behavior of these anchorage systems needs to be performed.

Anchorage systems for concrete structures can be divided into the two basic classifications: cast-in-place headed studs which are placed into the mould before concrete casting and post-installed anchors (undercut, expansion, adhesive etc.) which are installed into the hardened concrete (Fuchs *et al.*, 1995). The four modes of anchors failure subjected to tension can be identified for these anchorage systems: steel yielding, pulling-out, concrete splitting and concrete breakout (CEB-fib, 1997). This paper is focused on behavior of shallow cast-in-place headed stud and its concrete breakout capacity in dependence on the head size and effective depth of anchor especially. The other ways of failure or different types of anchors were not the objective of this paper. There have been done few experimental and numerical researches worldwide

that proved the influence of the head size on the breakout capacity of single anchor. Ožbolt *et al.*, (2006), simulated behavior of large embedded anchors (effective depth varied from 150 mm to 1500 mm) with three different head size types. He found that there is about 25% increase of capacity of medium sized head (31 mm) and about 35% increase of capacity of large sized head (40 mm) in comparison to small head (22 mm) for effective depth of 150 mm. The significant increase of capacity in dependence of head size was found also for the others effective depths.

## 2.0 Breakout Capacity Design

Two methods can be used for the calculation of breakout capacity of single anchor – concrete capacity design (CCD) and so called stress cone method (SCM). Fuchs *et al.*, (1995) showed that CCD approach can be used for prediction of anchor capacity, especially for shallow anchors up to 250 mm of effective depth (Cannon, 1995). The influence of the head size on breakout capacity of anchor is not involved in CCD approach which is adopted by Eurocode (BS EN 1992 -1-1, 2004) and ACI 318 (ACI committee 318, 2005) in comparison to SCM (Cannon, 1995) which considers the head size influence and is adopted by ACI 349 (ACI committee 349, 1988). Because the CCD method is involved in many world standards for calculation of breakout capacity, the emphasis is given on this method instead of SCM in this paper.

The CCD breakout capacity of single anchor is based on the presumption that the concrete fails in the shape of pyramid (Fig. 1) with the pyramid base equaled to three times effective depth ( $3h_{ef}$ ). This presumption corresponds to widespread experimental observations. The equation (1) is based on this prediction and can be used for calculation of breakout capacity of single anchor  $N_{n0}$  (Fuchs *et al.*, 1995):

$$N_{n0} = k_{nc} \cdot \sqrt{f_{cc}'} \cdot h_{ef}^{1.5}; \quad (1)$$

with:

$k_{nc}$  is 15.5 for mean value of cast-in-place anchors,  
 $f_{cc}'$  concrete cubic strength [MPa],  
 $h_{ef}$  effective depth of anchor [mm].

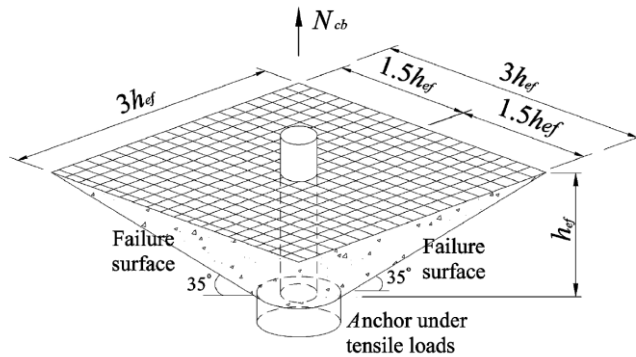


Figure 1: Idealisation of concrete breakout failure via CCD approach (ACI Committee 318, 2005).

### 3.0 Numerical Analysis

The commercial software ATENA (Advanced Tool for Engineering Nonlinear Analysis) was used for the solution of the problem. The GiD software was used as the pre- and post-processor. Material models for nonlinear behavior of concrete and steel were part of the used version of the ATENA software.

#### 3.1 Geometry of the Model

The twenty four 2D axi-symmetric models were created because the problem is typically axi-symmetric task (Pivonka *et al*, 2004). Variables of the simulations were effective embedment depth  $h_{ef}$  of anchor, diameter of head  $d_h$  and diameter of shank  $d_d$ . The head diameter was set in dependence on effective depth  $h_{ef}$ . Presence of anchor's shank was simulated by the spring attached to the side of concrete above the head. Shank diameter was set to theoretically avoid steel failure and was changing with effective depth. The dimensions of  $h_{ef}$ ,  $d_h$ ,  $d_d$  are specified in Tab. 1.

The axi-symmetric model consisted of two materials steel - anchor head, support ring and concrete block. The anchor head thickness was 10 mm for all simulations. The support ring's dimensions were set to 50 x 50 mm for almost all simulations except for  $h_{ef} = 200$  mm. In this case the support ring was 100 x 100 mm.

The concrete block's size varied in dependence on effective depth. The scheme of the geometry is shown in the Fig. 2 and the dimensions are stated in the Tab. 2. Concrete block (light grey) was divided into three parts because of different mesh density and dimension  $c$  was set to be larger than  $1.5h_{ef}$  to ensure the creation of concrete cone in fine mesh.

### 3.2 Material Models

#### 3.2.1 Steel model

The bilinear von Mises plasticity model was used for the modeling of steel head and of the support ring. The parameters of model are specified in the Tab. 3

#### 3.2.2 Concrete model

The fracture-plastic model Cementitious2 which is included in the ATENA software was selected for the numerical simulation of concrete. This model combines constitutive models for tensile (fracturing) and compressive (plastic) behavior. It employs Rankine failure criterion, exponential softening and it can be used as rotated or fixed cracks. The hardening/softening plasticity model is based on Menétrey-William failure surface. This model can be used to simulate concrete cracking, crushing under high confinement and crack closure due to crushing in other material directions (Červenka *et al.* 2009). The cubic compressive strength was set 30,0 MPa and it was kept constant during all the simulations. The basic parameters of the concrete model are stated in the Tab. 4.

Table 1: Dimensions of Numerical Model

$h_{ef}$	<b>a</b>	<b>b</b>	<b>c</b>	$h_{ef}/c$
[mm]	[mm]	[mm]	[mm]	[-]
90	425	500	250	2.8
120	425	500	300	2.5
150	500	500	350	2.4
200	600	600	450	2.25

Table 2 : Anchor Geometry in Dependence on Effective Depth

		$d_h/h_{ef}$					
		<b>0.2</b>	<b>0.25</b>	<b>0.3</b>	<b>0.35</b>	<b>0.4</b>	<b>0.45</b>
$h_{ef}$	$d_d$	$d_{h;0.2}$	$d_{h;0.25}$	$d_{h;0.3}$	$d_{h;0.35}$	$d_{h;0.4}$	$d_{h;0.45}$
[mm]	[mm]	[mm]	[mm]	[mm]	[mm]	[mm]	[mm]
90	13.5	18	22.5	27	31.5	36	40.5
120	18	24	30	36	42	48	54
150	22.5	30	37.5	45	52.5	60	67.5
200	30	40	50	60	70	80	90
$d_h/d_d$		1.33	1.67	2	2.33	2.67	3
$A_b/A_d$		1.77	2.79	4	5.43	7.13	9

Table 3 : Material Parameters of Steel

Parameter	Units	Value
Elasticity modulus E	[GPa]	210.0
Poisson coefficient $\nu$	[ - ]	0.3
Yield strength $f_y$	[MPa]	550
Hardening modulus H	[GPa]	10

Table 4: Material Parameters of Concrete

Parameter	Units	Value
Elasticity modulus E	[GPa]	30.32
Poisson coefficient $\nu$	[ - ]	0.2
Compressive strength $f_c$	[MPa]	-25.5
Tensile strength $f_t$	[MPa]	2.317

### 3.2.3 Boundary Conditions of the Model

The model was supported by the reaction  $R_y$  which was set on the support ring and by the axis of symmetry. The displacement  $w$  was gradually applied (in 40 – 80 steps) on the shank area of the head (Fig. 3) to simulate progressive loading. The maximum displacement varied from 1.0 mm to 8.0 mm in dependence of effective depth and head diameter (the smaller displacements were set for the large head diameters). The reaction  $R_y$  was monitored during the loading.

Small gap (1 mm) was created between the concrete block and the head on the side and on the bottom of the head to avoid the transfer of friction and tension from the head to concrete. The head was rigidly connected to the concrete block only on the top bearing area (Fig.3).

The spring constraint was set along the concrete block in place above the head of the anchor where the steel shank is normally present (Fig. 3). The spring was set in the perpendicular direction to the displacement (horizontal in global) to simulate presence of the shank and to allow the vertical displacement. Multi-linear stiffness  $k$  of the spring was selected to simulate the behavior of the spring. Spring behaved as concrete in tension and as steel in compression to prevent from pushing of concrete into the shank cavity.

### 3.2.4 Finite Element Discretization

The unstructured mesh was generated by automatic generator which is implemented in pre-processor. Fine mesh with size of elements about 5 mm or less was created in the area I. where the cracks of concrete were expected. In the closest vicinity to the head smaller (approx. 1 mm) elements were generated. The coarse mesh – element size between 25-50 mm – was created in the other areas of concrete block to save the calculation time. Typical mesh is depicted in Fig. 4.

## 4.0 Results of Numerical Analysis

The maximal achieved reactions against head size (ratio  $d_h/h_{ef}$ ) in comparison to CCD method are stated in Tab. 5. It can be observed that with increasing size of the head the capacity of the anchor increases significantly in all cases. The increase is more significant for the anchors with larger effective depth. There can also be seen the significant decrease (between 40 and 20 %) of the anchor capacity in comparison to the CCD method for small headed anchors.

Table 5: Maximal reactions in dependence of head diameter

		$d_h/h_{ef}$					
		0.2	0.25	0.3	0.35	0.4	0.45
$h_{ef}$	CCD	$R_{y,max}$					
[mm]	[kN]	[kN]					
90	72.5	47.4	56.8	69.5	72.1	75.1	80.3
120	111.6	79.7	101.3	110.4	126.3	125.7	132.2
150	156.0	111.6	154.6	174.4	181.2	184.3	202.1
200	240.1	186.5	250.8	277.8	304.4	324.6	345.7

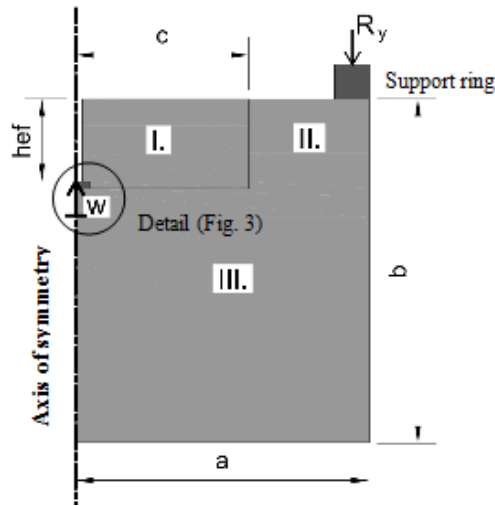


Figure 2: The scheme of numerical model geometry (light grey– concrete, dark grey– steel) .

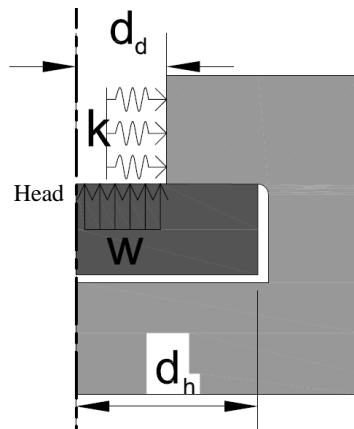


Figure 3: Detail of the anchor head (light grey– concrete, dark grey– steel).

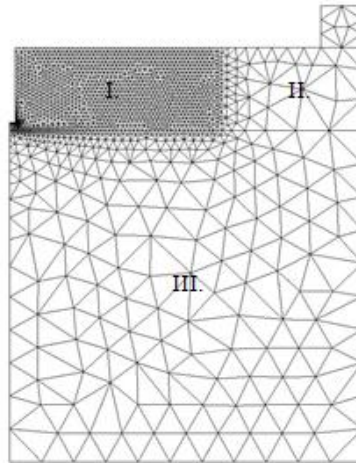


Figure 4: Typical mesh discretization

Typical diagram of reaction against displacement is shown in Fig. 5. All samples where  $h_{ef} = 120$  mm with different head diameters are compared in this diagram. The stiffer response of the anchor with increasing head size can be observed. This phenomenon was mentioned also in Ožbolt *et al.* (2006) and it was noticed for all other effective depths. The maximal reactions are pointed out in the diagram (grey dots).

The two basic modes of concrete cone failure were observed. Cracking mode (a) was observed mainly on the shallowest anchors and on the anchors with small head (Fig. 6). On the other hand the cracking mode (b) was observed mainly on the anchors with larger effective depth and with large heads (Fig. 7). The cracking in the mode (b) progressed in two phases: at first the bottom crack I. was established and then after maximum reaction was achieved the crack II. was formed and it was opening till the end of the simulation. The crack I. had not continued in progress after the crack II. opened.

At first the different modes of cracking were put in the connection with the relatively thin (10 mm) head thickness for large effective depths and large head sizes. It was found that almost 30 - 40 % of head cross-section plasticized in these cases. Hence the two new simulations ( $h_{ef} = 150$  mm,  $d_h/h_{ef} = 0.45$ ;  $h_{ef} = 200$ ,  $d_h/h_{ef} = 0.45$ ) were run with anchor thickness equals to 75% of shank diameter (only 0 - 4 % of cross-section plasticized) with almost the same results. The modes of cracking were very similar and anchor capacity almost the same in comparison to thin (10 mm) head. The response of simulations with thicker heads was slightly stiffer which is reasonable because none or minimal plasticity in the head occurred.



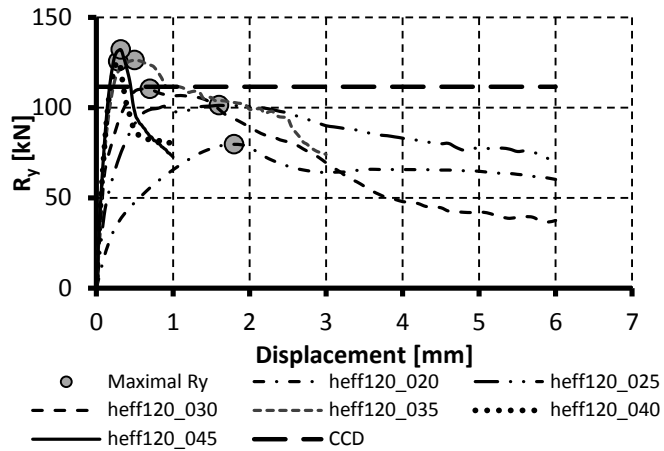


Figure 5: Typical diagrams of reaction against displacement in dependence on head size.

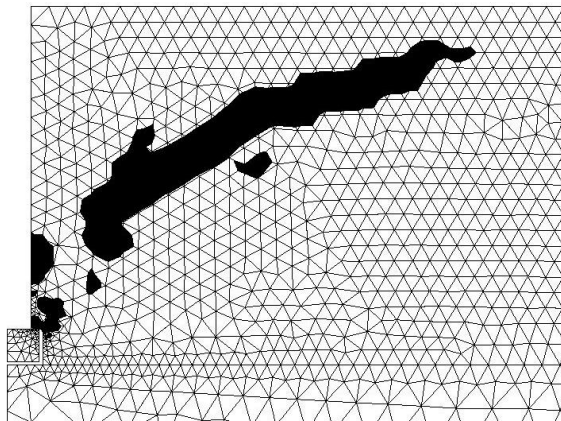


Figure 6 : Typical (a) mode crack (black) -  $h_{ef} = 90$  mm;  $d_h/h_{ef} = 0.2$ .

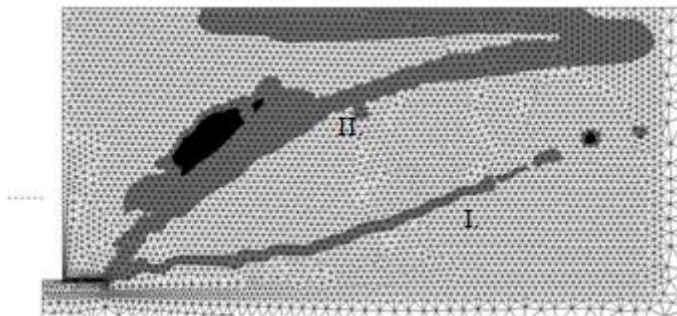


Figure 7 : Typical (b) mode crack (grey, black) -  $h_{ef} = 200$ ;  $d_h/h_{ef} = 0.45$

#### 4.1 Coefficient of head size influence

The bi-linear coefficient based on the numerical data which takes into account the influence of the head size was created. This coefficient results from the outcomes of simulation of the model -  $h_{ef} = 120$ ;  $d_h/h_{ef} = 0.3$ . This simulation was the closest to the CCD method prediction.

$$k_h = \left(\frac{h_{ef}}{120}\right)^{0.3} \cdot \left(\frac{d_h/h_{ef}}{0.3}\right) \quad \text{for } d_h/h_{ef} < 0.3 \quad (3)$$

$$k_h = \left(\frac{h_{ef}}{120}\right)^{0.3} \cdot \left(\frac{d_h/h_{ef}}{0.3}\right)^{0.5} \quad \text{for } 0.45 \geq d_h/h_{ef} \geq 0.3 \quad (4)$$

The use of equation (4) is limited to  $d_h/h_{ef} = 0.45$  because up to this values the simulations have not been executed. For the ratio larger than 0.45 the same value should be used (Fig. 8).

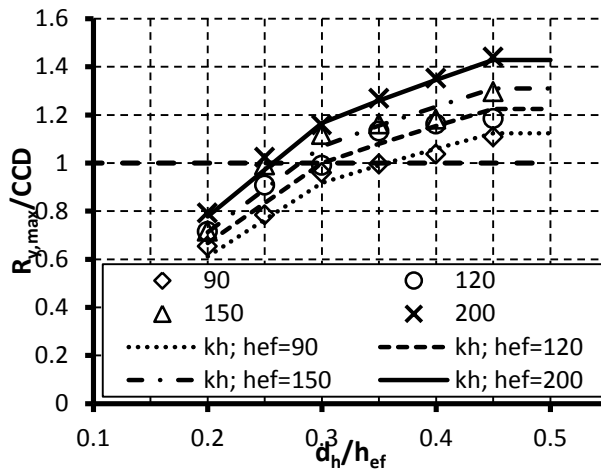


Figure 8 : Maximal reactions  $R_y$  and coefficient of head size influence  $k_h$ .

## 5.0 Conclusions

Twenty-four numerical simulations of headed studs with different effective depth and head diameter were carried out in this research. The findings can be summarized in the next four points:

- The simulations approved that size of the head has significant influence on the capacity of anchor in tension. It was found that for small heads of anchor can be the CCD approach unsafe and for large heads is this approach quite conservative.
- The stiffer response of the anchor can be observed with the increase of the head size. This phenomenon was observed within all simulations.
- The two different basic modes of concrete cracking were observed in dependence of head size and effective depth.
- Based on the numerical data the coefficient of head size influence  $k_h$  was created. This coefficient increases/decreases the capacity of anchor calculated according to the CCD.

It has to be stated that these findings are based only on theoretical numerical research. The more theoretical and mainly experimental research should be made to improve the validity of these findings and to refine the CCD approach.

### Acknowledgment

J. Fornůšek thanks to dr. John. J. Cairns from the Heriot Watt University for the patience and help with author's thesis. J. Fornůšek would like also thanks to the company Červenka Consulting Ltd. for providing of the student version of ATENA Science software.

### References

- ACI Committee 318, (2005), Appendix D – Anchoring to Concrete, *Building Code Requirements for Structural Concrete and Commentary*, ISBN-10: 9780870312649.
- ACI Committee 349 (1988), Code Requirements for Nuclear Safety Related Concrete Structures, American Concrete Institute, Detroit.
- BS EN 1992-1-1:2004, (2004), Eurocode 2: Design of concrete structures — Part 1-1: General rules and rules for buildings, British Standards Institute, London.
- Cannon R., (1995), Discussion to the paper Concrete Capacity Design (CCD) Approach for Fastening to Concrete, *ACI Structural Journal*, November - December, pp. 787-791.
- Cannon R., (1996), Straight Talk about Anchorage to Concrete – Part I, *ACI Structural Journal*, 92-S56, pp. 580-586.
- CEB-fib, (1997), Design of Fastening in Concrete: Design Guide, Thomas Telford, London, UK.
- Červenka V., Jendele L. and Červenka J., (2009), ATENA Program Documentation Part 1 - Theory, Červenka Consulting Ltd., Prague.
- Fuchs W., Eligehausen R. and Breen J.E., (1995), Concrete Capacity Design (CCD) Approach for Fastening to Concrete, *ACI Structural Journal*, 92-S9, pp. 73-94.

- Ožbolt J., Eligehausen R., Periškić G and Mayer U., (2007), 3D FE analysis of anchor bolts with large embedment depth, *Engineering Fracture Mechanics*, 74, pp. 168-178.
- Pivonka P., Lackner R and Mang H.A., (2004), Concrete Subjected to Tri-axial Stress States: Application to Pull-Out Analysis, *Journal of Engineering Mechanics*, December, pp. 1486-1498.